Chapter 18

Graphene Materials to Remove Organic Pollutants and Heavy Metals from Water: Photocatalysis and Adsorption

Eduardo E. Pérez-Ramírez,
Miguel de la Luz-Asunción,
Ana L. Martínez-Hernández and
Carlos Velasco-Santos

Additional information is available at the end of the chapter

http://dx.doi.org/10.5772/62777

Abstract

Since graphene was isolated from graphite, different researches have been developed around it. The versatility of graphene properties and their derivates, such as graphene oxide or doped and functionalized graphene materials have expanded the possible applications of these nanostructures. The areas studied of graphene include the following: nanocomposites, drug delivery, transistors, quantum dots, optoelectronic, storage energy, sensors, catalyst support, supercapacitors, among others. However, other important field of these materials is their applications in environment, mainly in the removal of pollutants in water. In this context, there are two possible alternatives to use graphene materials in water purification: photocatalysis and adsorption. In the first case, the key is related to the bandgap and semiconductors properties of these materials, also the versatility of different graphene structures after the oxidation or functionalization, play an important role to get different arrangements useful in photocatalysis and avoid recombination, one of the problems of typical semiconductors photocatalysts. In the second case, surface area and useful chemical groups in carbon material give different options to produce efficient adsorbents depending on different synthesis conditions. Thus, this book chapter covers a review of the photocatalytic activity of graphene materials with emphasis in the removal of organic pollutants and heavy metals from water, in the next topics: graphene-based semiconductor photocatalyst and graphene oxide as photocatalyst. On the other hand, the chapter also discusses the research related to the removal of organic compounds and heavy metals using graphene materials as adsorbents, the topics in this second part are as follows: graphene and graphene oxide as adsorbent of heavy metals from water, graphene, and graphene oxide as adsorbent of organic pollutants from water,

functionalized graphene materials as adsorbent of water pollutants, carbon nanomaterials vs. graphene as adsorbents. Therefore, the book chapter presents a review and the discussion of the keys that play an important role in the advances in the research of graphene materials as photocatalysts. In addition, the isotherms and kinetic that produce these materials as adsorbents are also reviewed and discussed, because adsorption process in these materials is important to remove pollutants from water, but also for adsorption is a first step to achieve photocatalyst. The future of this topic in graphene materials is also analyzed.

Keywords: Graphene, Graphene oxide, Photocatalysis, Adsorption, Water pollution

1. Introduction

Water demand has increased as a consequence of different human activities and industrial growth. Water resources are contaminated due to the discharge of wastewater. The discharge of industrial effluents uncontrolled, containing large amounts of contaminants, represents a danger for human beings and aquatic life. By the aforementioned, the water pollution is a worldwide problem, which represents a serious risk to the environment and water quality. Therefore, it is necessary to develop new methods and materials for removing contaminants from wastewater.

Several conventional methods have been reported in the literature to remove contaminants from water and wastewater; however, these methods have large disadvantages. Photocatalytic degradation has shown great potential in the treatment of water. It has many advantages over conventional methods. Semiconductor-based photocatalysis has received great attention due to its use in water purification. Some researchers have reported water splitting using semiconductor photocatalyst, and it has attracted a lot of attention in different fields of science.

Adsorption is also widely used to remove contaminants from industrial wastewaters. When compared to conventional methods, adsorption offers significant economic and environmental advantages such as low cost, ease of operation, and high removal efficiency.

At present, the application of nanomaterials in water treatment has attracted significant attentions for the advantages of large surface areas and activated functionalized sites. Nanomaterials are very attractive in different fields of the science and have gained great interest due to their adsorption, catalytic, optical, and thermal properties among others. Researchers in science and engineering show an increased interest in the use of nanoparticles due to their unique physical and chemical properties.

Research on graphene (GE) has experienced strong growth in recent years. Graphene materials have already made great impacts in many fields ever since its discovery in 2004. Graphene oxide (GO) is one of the most important graphene materials.

This kind of nanomaterials represents a new type of photocatalyst/adsorbent offering an alternative to remove specific contaminants from water. Due to this, in this chapter, we present

http://dx.doi.org/10.5772/62777

a review of investigation studies where graphene and graphene based materials have been used as photocatalysts and adsorbents for the removal of heavy metals and organic compounds from water. The effect of some parameters affecting the process of photocatalysis and adsorption is analyzed.

2. Photocatalysis of graphene materials to remove pollutants from water

Heterogeneous photocatalysis is an advanced oxidation process (AOP) that offers an important potential for the decomposition of recalcitrant organic pollutants of water. In this process, the photon energy is converted into chemical energy which is able for the decomposition of these contaminants. One of the challenges in the heterogeneous photocatalysis is to improve the charge separation for make more efficient the process. In this regard, graphene materials are very promising for solve the recombination process. The structures of graphene materials with sp^2 hybridization of carbon atoms can allow a fast electron transfer improving the charge separation. Therefore, in this section, we present a review of investigations about of the use of graphene materials and graphene-based materials for the organic pollutants removal of water through of photocatalysis process.

2.1. Graphene-based semiconductor photocatalysts

With the aim to improve the performance of photocatalytic semiconductors materials, some strategies have been employed. One of the combinations of these semiconductors materials are with graphene. This nanomaterial can serve as an electron acceptor and therefore to improve the charge separation.

Although titanium supported over graphene materials is the most studied semiconductor on the removal of organic pollutants from water [1–4], exist other semiconductors that have been incorporated to graphene layers, in order to observe the modification of its effect on the removal of organic pollutants of water. This chapter section will be focused on making a review of semiconductors of oxides and sulfides which have had important impact when these are incorporated to the graphene materials.

Cuprous oxide (Cu_2O) is one of the more important semiconductors that have been combined with graphene materials. Han [5] investigated the performance of nanocomposite of Cu_2O–reduced GO (Cu_2O–RGO) on the photodegradation of methylene blue under visible light. The results showed an important increase of the photocatalytic activity of the Cu_2O–RGO nanocomposites respect to Cu_2O nanoparticles. This enhancement of the nanocomposites was attributed to the enhanced light absorbance, the extended light absorption range and a more easy transfer of photogenerated electrons of Cu_2O to RGO getting better charge separation which was corroborated by photoluminescence. Similar results have been found by Zhigang [6] and Sun [7] on the rhodamine B degradation where the enhanced photocatalytic activity was attributed to the strong interaction between Cu_2O and RGO nanosheets. Zou [8] synthesized Cu_2O–RGO composites for the methylene blue degradation under visible light finding that the photocatalytic activity of the composites was influenced by the Cu_2O crystal facet,

being the {111} facet that exhibited the enhanced visible light absorption and faster charge-transfer rate. Besides, the catalytic activity of the Cu_2O–RGO composites was related to the interfacial interactions and electronic structures.

Other semiconductor that has been combined with graphene materials is zinc oxide (ZnO). Tayyebi [9] decorated GO with zinc oxide quantum dots (QDs) by a chemical method for degradation of methyl orange in water. Strong interaction between ZnO and GO were found through C–O–Zn and C–Zn bridges. Besides, the adsorption range of visible light was increasing. The bandgap decreased of 3.1 eV in ZnO QDs to 2.8 and 2.9 eV in ZnO-10% graphene and ZnO-5% graphene, respectively. These hybrids of ZnO–graphene showed a better performance on the degradation of methyl orange that ZnO QDs. The increasing of the photocatalytic activity of the hybrids was attributed to the reduction of electron–hole recombination rate, the extended absorption of visible light, and the high surface area of graphene. Similar behavior was found by Rabieh [10]. The ZnO–RGO composites achieved a 99% of efficiency on the azure B dye degradation after of 20 min of reaction. The photocatalytic activity of ZnO–RGO composites was increased with the increasing of graphene. Other composites of graphene–ZnO with different morphologies have been synthesized by different methods showing good results on the organic pollutants degradation in water [11,12]. **Figure 1** shows a schema of the transfer of photogenerated electrons from a metallic oxide to graphene.

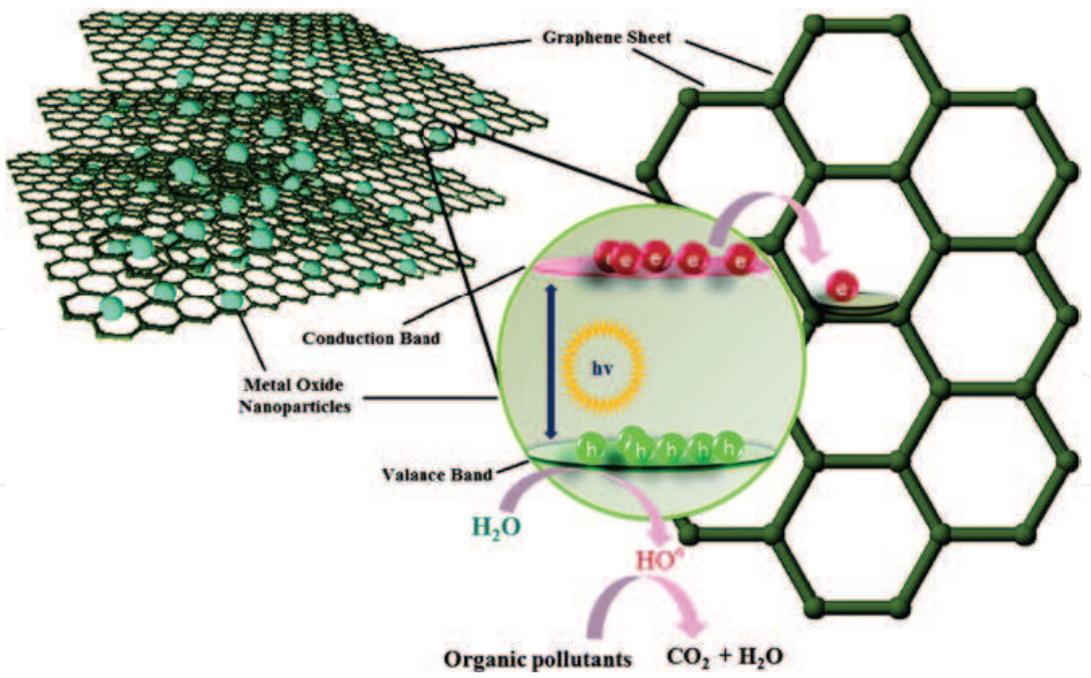

Figure 1. Schema of the mechanism of electron transfer from conduction band of metal oxide to graphene sheets. Reproduced with permission from Upadhyay et al. [13]. Copyright ©2014, The Royal Society of Chemistry.

In addition to metallic oxides, metal sulfides have also been combined with graphene searching photocatalysts with a higher photocatalytic activity for the organic contaminants degrada-

tion in water. Chakraborty [14] reported the synthesis of RGO–ZnS composites for optoelectronic device. The photocatalytic activity of the composite was proved on the rhodamine B under UV light irradiation for 4 h, getting a degradation efficiency of 84, 34% more than ZnS nanorods. The same composite was used for four cycles showing a constant degradation efficiency of rhodamine B. Composites of CdS and RGO were synthesized by Zou [15]. The photocatalytic activity of the RGO–CdS composites on the Congo red dye degradation improved the efficiency obtained with CdS, reaching a efficiency of 90% which was attributed to the RGO performance as an effective acceptor electron.

Ternary systems such as RGO–TiO_2–ZnO [16] and RGO–TiO_2–Cu_2O [17] have been synthesized and employed successfully as photocatalysts for the degradation of organic pollutants of water. Other compounds with graphene that have been used are GO–Ag_2CO_3 [18], GO–Ag_3PO_4 [19,20], and RGO–$BiPO_4$ [21].

2.2. Graphene oxide as photocatalyst

GO is a functional form of graphene containing oxygenated groups. The basal plane of GO is covalently surrounded by the hydroxyl and epoxy groups, while carboxyl groups are found in the edges of the sheets [22]. These oxygenated groups make of the GO a hydrophilic material, improving the dispersion in water. Its bandgap can be adjusted modifying the level oxidation [23]. The easy dispersion in water and its tunable bandgap motivate to explore this material for applications in the photocatalysis area [24].

The photocatalytic activity of GO has been reported in some investigations. Krishnamoorthy [24] reported the photocatalytic properties of GO nanostructures. The photocatalytic activity was evaluated through of the resazurin (RZ) reduction as a function of irradiation time under UV light of 350 nm. The bandgap of GO was calculated to be 3.26 eV. In the photocatalytic experiments were used 10 mL of resazurin solution at a concentration of 1.5 mg/L and different concentrations of GO (0.5, 0.75, and 1 mg). Results showed the reduction of RZ into resorufin (RF) which was corroborated by the color change from blue into pink and the change in the bands adsorption of the adsorption spectra (**Figure 2**). The reduction of resazurin into resorufin was well fitted to pseudo-order reaction. The reduction of resazurin was attributed to the photoexcited electrons from the surface state of GO caused by the UV irradiation.

Aromatic compounds as phenol and 4-chlorophenol have been removed of water using GO as photocatalyst [25]. In the experiments for the removal of phenol were employed 100 mL of phenol solution at a concentration of 100 mg/L. The concentrations of GO were 100 and 200 mg/L and was used an UV lamp of 254 nm. The maximum removal achieved was 38%. The photocatalytic activity was influenced by the deggasing units used in the preparation of GO samples [26]. A major photocatalytic activity of GO was found on the degradation of 4-chlorophenol in water. 30 mL of 4-chlorophenol solution at a concentration of 30 mg/L were used in the experiments. The concentration of GO was 0.8 g/L. 97% of the 4-clorophenol was eliminated after of 120 min of reaction. The chemical oxygen demand (COD) results showed that up to 97% of organic matter was removed.

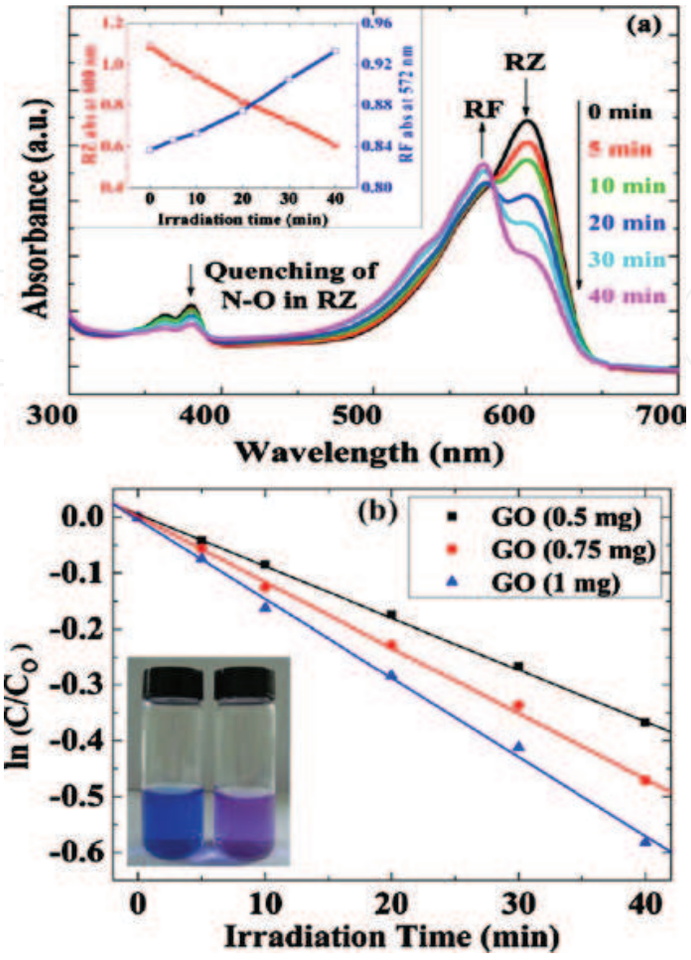

Figure 2. (a) Reduction of RZ into RF catalyzed by 1 mg of GO with respect to time. (b) Influence of the catalyst concentration (GO) on the reduction process of RZ into RF. Inset: Image of the GO–RZ solution before (left) and after (right) UV exposure. Reprinted with permission from Krishnamoorthy et al. [24]. Copyright ©2011, AIP Publishing LLC.

In addition to decontamination of water, GO promises good results as photocatalyst for hydrogen production from water and for CO_2 to methanol conversion. Yeh [23] confirmed the photocatalytic activity of GO through the generation of H_2 from water. For the experiments was used a glas-closed circulation system with inner irradiation. The mercury lamp used consists of both UV and visible light. The reactions were conducted in pure water and 20% volume aqueous methanol. The methanol in the solution reduced the recombination increasing the amount of H_2 produced. The high dispersion in water of GO induced that the carbon atoms on the sheets were accessible to protons that could be transformed to H_2.

The CO_2 to methanol conversion was studied by Hsu [22]. The experiments of photocatalytic reduction of CO_2 in gas phase were carried out under ambient conditions using a halogen lamp as irradiation source. Modified Hummers method was employed for the synthesis of three GO samples. The samples GO-1, GO-2, and GO-3 corresponding to the traditional form, excess of $KMnO_4$ and excess of H_3PO_4, respectively. The results obtained with this three samples of GO were compared with the results obtained with the commercial TiO_2. The order of methanol

formation was found to be as follows GO-3 > GO-1 > GO-2 > TiO_2 (P-25). The good performance of GO-3 was attributed to the excess of H_3PO_4 which improved the protection of the GO basal plane. The modulation of oxygenated functional groups is an important control parameter. In addition to the CO_2 reduction, GO can be simultaneously used for the solar energy harvesting.

3. Graphene materials as adsorbents

In this section, graphene, graphene oxide and reduced graphene oxide were analyzed as adsorbent to study the adsorption characteristics of heavy metal compounds and organic from aqueous solutions. Some concepts about the kinetics and isotherms adsorption are provided. Otherwise, some researchers have suggested carbon nanotubes (CNT) and oxidized carbon nanotubes (OCNT) as adsorbents with good adsorption capacity. Thereby, subsequently, we include a discussion about the comparison between CNT and graphene materials.

The main emphasis is on the description relevant experiments and important results as well as some of the novel applications of graphene materials as adsorbents. We include a summary of current experimental work that has been done in the area of graphene materials on adsorption process. In the end of the chapter is presented a comparison of adsorbents derived from graphene materials versus others carbon nanomaterials (CNM).

At present, carbon-based porous materials assembled by two dimensional (2D) such as GE, GO, and RGO have attracted a great attention as effective pollutant adsorbents owing to their high adsorption capacities and rapid adsorption rates [27]. However, search for novel and efficient adsorbents for the removal of contaminants from wastewater is imperative.

Researchers have tested many different types of developed adsorbents such as activated carbon (AC), zeolite and polymer, nanoparticles and nanocomposites, and other adsorbents are used for the removal of impurities from the aqueous solution. However, these adsorbents have been suffering from either low adsorption capacities or low efficiencies. Therefore, great effort has been made in recent years to seek new adsorbents and develop new techniques [28]. Many papers have been published in the past few decades, confirming that the carbonaceous materials are effective adsorbents for decontamination from wastewater. Their high sorption capacities are associated with the large specific surface area and the existence of a wide spectrum of surface functional groups [29]. Nanomaterials have been studied for the absorption of metal ions and organic compounds. Although it was discovered just a few years ago, GE and its derivates have attracted tremendous research interests not only in electronics and energy fields, but also in environmental applications [30]. The inherent advantages of the nano-structured adsorbent, such as adsorption capacity, easy and rapid extraction, handy operation, and regeneration, may pave a new, efficient, and sustainable way toward highly-efficient pollutant removal in water and wastewater treatment [31].

CNT, as member of the carbon family, have attracted special attentions to many researchers after their discovery in 1991, because they possess unique morphologies and have showed excellent properties and great potential for engineering applications. CNT are also good anion

and cation adsorption materials for wastewater treatment, as they exhibit exceptionally large specific surface areas [32]. Their layered nanosized structures make them a good candidate as absorbers [33].

Similarly, GE consisting of 2D hexagonal lattices of sp^2 carbon atoms covalently bonded has been theorized to have a huge specific surface area (over 2600 $m^2\ g^{-1}$), leading to its potential in the environmental field as an effective choice for pollutant elimination or environmental remediation [34]. Graphene is hydrophobic and, consequently, stable dispersions in polar solvents can only be obtained with addition of proper surfactants. GO is similar to GE, but presents oxygen-containing functional groups such as hydroxyl and epoxide (mostly located on the top and bottom surfaces), and carboxyl and carbonyl (mostly at the sheet edges), randomly distributed in the graphene structure [28,34]. These functional groups markedly increase the hydrophilicity of GO, making it easily dispersible in aqueous solution and stable under common environmental conditions [35]. These functional groups can interact with positively charged species such as metal ions, polymers, and biomolecules [36].

CNT, GE, and GO are newly emerged carbonaceous nanomaterials, their characteristic structures and electronic properties make them interact strongly with organic molecules, via non-covalent forces, such as hydrogen bonding, π–π stacking, electrostatic forces, van der Waals forces, and hydrophobic interactions. Their nanosized structures also endow them some advantages such as rapid equilibrium rates, high adsorption capacity, and effectiveness over a broad pH range [37]. All these advantages suggest that CNM are promising adsorbents for environmental protection applications [38].

Parameters such as pH, adsorbate concentration, type of chemical specie, and agitation among others influence in the adsorbent–adsorbate interaction. Some properties of the adsorbents that affect the adsorption process are specific surface area, pore size, and surface functional groups.

The pH is the most important factor affecting the adsorption process. The solution pH can affect the surface charge of the sorbent and the dissociation of functional groups on the active sites of the adsorbent as well as the adsorbate speciation [31]. The pH at which the positive and negative charges are balanced, and no net charge is available on nanomaterials surfaces, is called point of zero charge (PZC) [39]. The adsorbent surface is positively charged at pH values below the pH_{PZC} and negatively charged at pH values above the pH_{PZC} [29].

3.1. Kinetics of adsorption

Adsorption process generally involves four different steps. They are (a) external mass transfer in bulk liquid phase, (b) boundary layer diffusion, (c) intraparticle mass transfer within particle, and (d) sorption on active sites. However, out of the four steps, the effect of boundary layer diffusion and sorption on active sites on the adsorption kinetics is negligible whereas external mass transfer and intraparticle mass transfer affect the kinetics considerably [36].

Many models have been extensively applied in batch reactors to describe the transport of adsorbates inside the adsorbent particles, such as the pseudo-first order and the pseudo-second order equation, the Elovich and Intraparticle diffusion equation [40] (**Table 1**).

Kinetic model	Equation	Nomenclature	References
Pseudo-first order	$\log\left(q_e - q_t\right) = \log q_e - \frac{k_1}{2.303} t$	Where q_e and q_t (mg/g) are the amounts of adsorbate adsorbed at equilibrium and at time t, respectively, and k_1 (min^{-1}) is rate constant of pseudo-first order	[41]
Pseudo-second order	$\frac{t}{q_t} = \frac{1}{k_2 q_e^2} + \frac{1}{q_e} t$	Where, q_e and q_t have the same meaning as before, and k_2 is the pseudo-second order rate constant [g/(mg min)]	[27]
Elovich	$q_t = \frac{1}{\beta} \ln\left(\alpha\beta\right) + \frac{1}{\beta} \ln t$	Where q_t is the adsorbed phenol (mg/g) at time t (min), α is the initial adsorption rate [mg/(g min)] and β is related to the activation energy for chemisorption (g/mg)	[42]
Intraparticle diffusion	$q_t = k_{id} t^{1/2} + \theta$	Where k_{id} is the intraparticle diffusion rate constant (mg/g $min^{1/2}$), and θ represents the value of the thickness of the boundary layer (mg/g)	[43]

Table 1. Kinetic models reported in the literature.

Isotherm model	Equation	Nomenclature	References
Langmuir	$q_e = \frac{q_{max} K_L C_e}{1 + K_L C_e}$	Where q_e is the adsorption capacity of the adsorbate per unit weight of adsorbent (mg/g), q_{max} is the maximum adsorption capacity (mg/g) and K_L is the constant related to the free energy of adsorption (L/mg), C_e the equilibrium concentration of the adsorbate (mg/L)	[44]
Freundlich	$q_e = K_F C_e^{1/n}$	Where q_e is the equilibrium amount of the adsorbate per unit mass of adsorbent (mg/g), C_e the equilibrium concentration of the adsorbate (mg/L), K_F the constant indicative of the relative adsorption capacity of the adsorbent (mg/g $(L/mg)^{1/n}$), $1/n$ the constant indicative of the intensity of the adsorption	[45]

Table 2. Langmuir and Freundlich isotherm models.

3.2. Adsorption isotherm

Adsorption isotherm is the relationship between adsorption capacity and concentration of the remaining adsorbate at constant temperature [37]. That is, it indicates the relationship between the absorbent and the adsorbate when the adsorption process reaches an equilibrium state [39]. The adsorption process may be generally modeled by Langmuir and Freundlich isotherms.

However, other models, such as BET, Tempkin, and Toth, are also used. The Langmuir model assumes that the adsorption occurs on a homogenous surface and no interaction between adsorbates in the plane of the surface. The Freundlich equation is an empirical equation based on adsorption on a heterogeneous surface [40]. The parameters obtained from the models provide important information on the sorption mechanism and the surface property and affinity of the adsorbent [37] (**Table 2**).

3.3. Graphene and graphene oxide as adsorbent of heavy metals from water

The discharge of effluents has increased due to industrialization. Heavy metals in the water pose risks to health and cause harmful effects to living organisms in aquatic life. In contrast to organic compounds, heavy metals are not biodegradable. Effluents from industrial wastewater include chromium, arsenic, zinc, cobalt, mercury, cadmium, lead, and so on. Even at low concentrations, these metals can be toxic and carcinogenic to organisms. Several physical and chemical methods have been used to remove metals and organic compounds, such as filtration, chemical precipitation, coagulation, solvent extraction, biological systems, electrolytic processes, reverse osmosis, oxidation, and ion exchange [38]. However, these methods present low removal efficiency. Adsorption process is the most widely used method for water treatment due to its low cost, ease of operation, efficiency in treatment [46], environmentally friendly [47], and adsorbents can be regenerated through a desorption process. Besides, adsorption does not generate the formation of harmful substances [48].

Ren [29] presented a comparative study of Cu(II) decontamination by three different carbonaceous materials, such as GO, multiwalled CNT (MWCNT), and AC. Cu(II) adsorption on the carbonaceous materials as a function of pH and Cu(II) ion concentration was investigated. The PZC values of carbonaceous materials decrease in the order of PZC(GO) < PZC(AC) < PZC(MWCNT). The carbonaceous surface is positively charged at pH values below the PZC and negatively charged at pH values above the PZC. GO has the lowest PZC value and the maximum adsorption efficiency, followed by AC, and then MWCNT, suggesting that GO is a promising material for the removal of Cu(II) ions from aqueous solutions in acidic wastewater treatment.

GO was prepared via modified Hummers' method by Wang [49] to remove Zn(II) ions from aqueous solutions. Results indicated that the optimum pH for Zn(II) removal was about 7.0. The Fourier Transform Infrared analysis indicated the presence of oxygen-containing functional groups on the surface of GO. The q_e values, calculated by pseudo-second order model, represent a fine agreement with the detected values in experiment. Adsorption isotherm can provide the most important parameter for designing a desired adsorption system. The values of 'n', obtained from Freundlich isotherm, are larger than 1 and decrease as the temperature increases. These values indicate the favorable nature of adsorption at lower temperature. Langmuir isotherms fit better with experimental data than Freundlich isotherms. This result suggests that Zn(II) adsorption on GO may be monolayer. The adsorption–desorption experiments were performed to investigate the possibility of recycling of GO and recovery of Zn(II) ions. The desorption percentages of Zn(II) from GO are 91.6, 73.4, and 53.2% employing 0.1 M HCl, 0.1 M HNO_3, and H_2O, respectively.

Recently, Tan [50] synthesized GO membranes and were used as adsorbents for the removal of Cu(II), Cd(II), and Ni(II). The maximum adsorption capacities for Cu(II), Cd(II), and Ni(II) were 72.6, 83.8, and 62.3 mg/g, respectively. The adsorption reached an equilibrium state in a short time (10–15 min) owing to a larger interlayer spacing of the GO membranes, which is favorable for facilitating the interstitial diffusion of heavy metal ions to active sites. The GO membranes were regenerated more than six times, with a slight loss in the adsorption capacity.

The adsorption kinetics and isotherms of Cr(III) on GO has been studied by Yang [51]. According to thermodynamic parameters calculated, the adsorption of Cr(III) on GO was spontaneous and endothermic. The maximum adsorption capacity of Cr(III) on GO at pH 5.0 and T = 296 K was 92.65 mg/g, which was higher than other reported adsorbents. The number of negatively charged sites increased on the surface of GO with increasing pH, whereby the adsorption of Cr(III) was favorable. In this study, oxygen-containing functional groups on GO played an important role in the adsorption of Cr(III). Results suggest that GO was a suitable material for the removal of Cr(III) from water.

GO was used by Madadrang [52] to investigate the adsorption and desorption behavior on Pb(II) removal. Boehm's titration method was used to determine the amount of functional groups on the GO surface. Pb(II) reacts with these functional groups on GO surface to form a complex. The BET surface area of GO was determined to be 430 m^2/g. The time required to reach the equilibrium state with a sonication treatment was 5–15 min. This time is much shorter than AC and other carbon-based adsorbents, these results show the GO as an available product for the waste treatment.

GO was utilized as adsorbent by Yari [53] for the removal of Pb(II). In this work, the equilibrium time adsorption on GO surface was 60 min. This time is greater than the work reported by Madadrang [52], which was carried out at different conditions. In this study, adsorption capacity of Pb(II) on GO surface increased with increase in the temperature of surrounding, the adsorption capacity increases from 15.9 to 19.7 mg/g when the temperature increased from 288 to 308 K. This result shows the endothermic nature of Pb(II) adsorption on GO. Therefore, higher temperatures favor adsorption. The value of $\Delta H°$ was 22.70 (kJ/mol) from GO. Thus, this result indicate that adsorption Pb(II) on GO surface was a physisorption. A thermodynamic study was carried out, the results indicate that the adsorption of Pb(II) ion on GO surface was spontaneous and endothermic. A review about of heavy metals removal by graphene materials is shown in **Table 3**.

Adsorbent	Adsorbate	T (°C)	pH	Model used	References
GO	Zn	20, 30, 45	2–10	Langmuir Pseudo-second order	[49]
GO	Cu, Cd, Ni	30	2–7	Langmuir Pseudo-second order	[50]
RGO	Cd	25, 45, 65	2–9	Langmuir Pseudo-second order	[54]

Adsorbent	Adsorbate	T (°C)	pH	Model used	References
GO	Cr	23, 33, 43	3–8	Langmuir Pseudo-second order	[51]
GO	Cu	30	3–10	Langmuir	[29]
GO	Pb	25	2–8	Langmuir	[52]
GO	Pb	15, 25, 35, 45	2–9	Langmuir Type I	[53]

Cd, Cadmium; Cr, Chromium; Cu, Copper; Ni, Nickel; Pb, Lead; Zn, Zinc.

Table 3. Graphene materials as adsorbents for removal of heavy metals.

3.4. Graphene and graphene oxide as adsorbent of organic pollutants from water

The organic compounds have been widely employed in a large number of industries, such as paper making, coating, chemical, pharmaceutical, petroleum refining, leather, and textiles, among others. Discharges of these compounds on effluents have caused serious problems in water bodies. Dyes and phenolic compounds are two of the most important contaminants of water. These are harmful to aquatic organisms and human beings [31,55]. The complex aromatic structures of dyes make them more difficult to remove [40]. Phenols and their derivatives are well known for their biorecalcitrant and acute toxicity [56]. The removal of organic contaminants in water resources not only protects the environment itself, but can also stop the toxic contaminant transfer in food chains. Due to these harmful effects, they must be removed from wastewater discharge before releasing into the environment [28]. The necessity of remove the organic contaminants of water has generated the search of effective alternatives for solve this problem. The use of graphene materials as adsorbent for decontamination of water promises to generate good results. Different investigations of adsorption of organic contaminants onto graphene materials have been reported.

GO, RGO, and GE have been developed and investigated for their use on the removal of organic pollutants in aqueous solution. Kim [27] reported adsorption behavior of acid red 1 (AC1) and methylene blue (MB) dyes on RGO. The equilibrium adsorption time of MB onto RGO was around 10 min, while the equilibrium adsorption of AC1 was reached to a time of 800 min. The surface charge of RGO and the structure of dye molecules had an important influence in the adsorption capacities and the equilibrium adsorption times. The adsorption of MB onto RGO was due to electrostatic interactions and π–π interactions. On the other hand, π–π interactions and hydrogen bonding were responsible for the adsorption of AC1 onto RGO. **Figure 3** shows the interactions presents in RGO-MB (a) and RGO-AC1 (b) systems. The negative charge of the surface oxygenated groups of GO favored the fast adsorption of MB cationic dye through of electrostatic interactions. A similar behavior of MB adsorption onto GO was found in other works [30,37,39]. In other investigation on the MB removal by RGO, Liu [40] found that with increasing RGO dose the removal of MB increased but the MB adsorption capacity decreased. This decrease in the MB adsorption capacity is because only a part of the active sites of RGO are available for the adsorption of MB when the RGO dose

increased. The pH solution had no significant impact on the removal of MB. At pH = 3, the removal of MB was 85.95%; while at pH = 10, the removal reached 99.68%. When the temperature was increased from 293 to 333 K, the adsorption capacity of MB increased from 153.85 to 204.08 mg/g. The equilibrium data were better fitted to the Langmuir isotherm model than the Freundlich model which is agreed with the reported by other authors [27,37,39]. The oxidation degree of GO can increases greatly the adsorption capacity of MB and adsorption behavior would change from Freundlich-type to Langmuir-type [57].

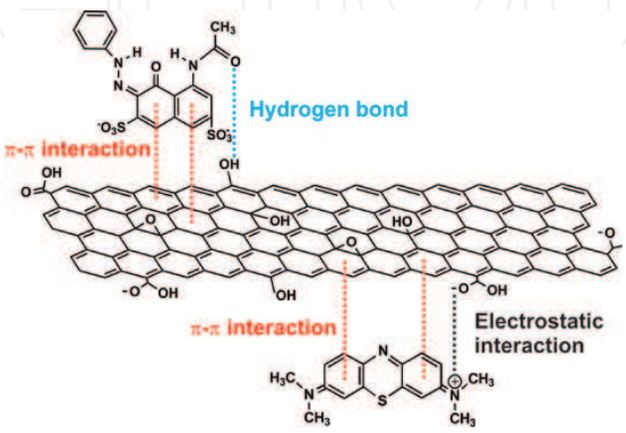

Figure 3. Scheme of interactions between RGO and AC1 dye molecules (up) and RGO and MB dyes molecules (down). Adapted with permission from Kim et al. [27].

The feasibility of using GE and GO as adsorbents for the removal of two toxic cationic dye basic red 12 (BR 12) and basic red 46 (BR 46) from aqueous solution was explored by Moradi [28]. The adsorption capacity of BR 12 and BR 46 increased with increasing of pH from 2 to 9. The major changes were observed in the adsorption of dyes onto GO. The changes on removal of dyes were very light when GE was used as adsorbent. This same behavior was found when was studied the effect of contact time. The order of removal of MB was as follows: GO-BR12 > GO-BR46 > GE-BR12 ≈ GE-BR46. The removal percentage of dye increased with increasing in the initial dye concentration. The adsorption of BR 12 onto RGO and GO indicate that the adsorption process was endothermic while the adsorption of BR 46 onto RGO and GO was an exothermic process. The results of adsorption of both cationic dyes indicated that the removal was more effective using GO as adsorbent, which was attributed to the surface oxygenated groups. Similar behavior of results had the experiment reported by Elsagh [46] on the removal of BR 46 onto GE and GO. In the adsorption process, the physisorption was found to be the main adsorption mechanism. The equilibrium adsorption data were best fitted to the Langmuir model and the adsorption kinetic data were well fitted to pseudo-second-order model.

The ability of RGO and GO to adsorb dyes such as methylene blue, methyl violet (MV), rhodamine B (RB), and orange G (OG) from aqueous solutions was studied by Ramesha [36]. GO showed an important affinity for the cationic dyes (MV and MB) reached the removal efficiencies up to 95%, while the adsorption of anionic dyes (RB and OG) was very low. On the other hand, RGO had better removal efficiency on anionic dyes than anionic dyes. The

removal efficiencies of RGO for anionic dyes were about of 95% while it were of 50% for cationic dyes. In the GO–MV and GO–MB systems, the adsorption was attributed to the electrostatic interactions, while the GO–OG system was mainly favored by the van der Waals interactions. In the GO–RB system, the interactions present are probably both electrostatic and van der Waals type. The adsorption process was found to follow pseudo-second-order kinetics in all the cases.

The removal of phenol from aqueous solution by RGO was studied by Li [55]. The adsorption of phenol onto RGO was studied in the pH range from 2.3 to 11.5. The best results of adsorption capacity were found in the pH range from 4 to 6.6. This was attributed to the surface functional groups which increased their surface complexation capability and π–π interactions between the aromatic ring of phenol and the aromatic structure of RGO. The percent removal of phenol was increased with increasing of the RGO dosage from 0.5 to 1.7 g/L but the adsorption capacity decreased. The pseudo-second-order equation was well fitted to the adsorption data. The adsorption isotherm data were well fitted by both Freundlich and Langmuir models. Thermodynamic study showed that adsorption of phenol onto RGO was endothermic and spontaneous process. In other work, the removal of 4-Chloro-2-nitrophenol (4C2NP) from aqueous solutions was performed using graphene as adsorbent [58]. Effect of the pH solution, contact time, initial concentration and temperature on the adsorption of 4C2NP onto GE was studied. The adsorption capacity of GE decreased with increasing dosage, but in all cases, the adsorption of 4C2NP by GE increased in the first 10 min and then achieved equilibrium at about 60 min. The higher adsorption of 4C2NP by GE was achieved in the pH range from 3 to 7. When the pH > 7 the adsorption of 4C2NP decreased. The adsorption of 4C2NP onto GE was increased with increasing the initial 4C2NP concentration from 2 to 10 mg/L. The opposite effect on the adsorption of 4C2NP was found when the temperature was increasing from 298 to 328 K. The adsorption kinetic data were best fitted to pseudo-second-order model, and the isotherm data were well described by the Freundlich isotherm model. Thermodynamic study indicated that the adsorption of 4C2NP onto GE was feasible, spontaneous, and exothermic in the temperature range from 298 to 328 K.

In addition to the dyes and phenols, others organic contaminants have been removed of water using GO as adsorbent. Pavagadhi [59] investigated the removal of two algal toxins, microcystin-LR (MC-LR) and microcystin-RR (MC-RR) from water. The adsorption kinetic of MC-LR and MC-RR onto GO was reached within 5 min with a removal major than 90% at the doses of 500, 700, and 900 μg/L. The adsorption capacity of GO was higher than AC. Due to their fast adsorption which is a very important parameter for design of water and wastewater treatment system, GO is a promising adsorbent for effective removal of MC-LR and MC-RR.

The adsorption of diclofenac (DCF) and sulfamethoxazole (SMX) onto GO in aqueous solution was reported by Nam [60]. Hydrophobic interactions and π–π electron donor acceptor were found to be the main adsorption mechanism of DCF and SMX onto GO. Both compounds reached the equilibrium within 24 h. The removal of DCF and SMX at equilibrium states were 50 and 12%, respectively, at a GO concentration of 100 mg/L. The sonication process had an important role on the removal of DCF and SMX. The removal percentage increased from 34 to 75% for DCF and from 12 to 30% for SMX. This was attributed to the reduction of

oxygenated groups on the surface of GO due to the increase in the sonication time which reduce the negative surface charge of GO and reduce the repulsion with the anionic compounds. The adsorption equilibrium data of DCF and SMX onto GO were fitted by the Freundlich isotherm. **Table 4** shows a summary of the results of adsorption of contaminant organics in water onto graphene materials.

Adsorbent	Adsorbate	T (°C)	pH	Model used	References
RGO	AC1	–	7	(MB) Langmuir	[27]
	MB			(AC1)Freundlich	
				Pseudo-second order	
G	MB	20, 40, 60	3–10	Langmuir	[40]
G	BR 12	20–40	2–9	Pseudo-second order	[28]
GO	BR 46				
GO	MB	20	2–9	Langmuir	[37]
				Pseudo-second order	
G	BR 46	20–40	2–9	Langmuir	[46]
GO				Pseudo-second order	
RGO	MB	ambient	2–10	(RB) Freundlich	[36]
GO	MV			Langmuir	
	OG			Pseudo-second order	
	RB				

AC1, acid red 1; BR 12, basic red 12; BR 46, basic red 46; MB, methylene blue; MV, methyl violet; OG, orange G; RB, rhodamine B.

Table 4. Comparison of graphene materials as adsorbents for removal of organic compounds.

3.5. Functionalized graphene materials as adsorbent of water pollutants

In an effort to improve the graphene and GO efficiency and overcome the limitations of these on the removal of the different pollutants in water, these materials have been functionalized with different organic groups. Some limitations for the use of GO are the high water absorption and the poor performance of the solid–liquid separation [61]. It will cause a risk of exposure to humans, animals, and aquatic organisms if GO remains in the filtered water [62,63]. Also, the functionalization of graphene materials can facilitate its dispersion and stabilization to prevent agglomeration [64]. Different functional groups such as carboxyl groups [65], hydroxyl groups [66], sulfhydryl groups, and amine groups [67] tend to have affinity by organic and inorganic pollutants as dyes and metals ions which are very important to achieve good removal efficiency. Different studies of heavy metal ion and dyes adsorption have been reported using as adsorbent functionalized graphene materials.

Wu [61] reported the removal of methylene blue employing a rhamnolipid-functionalized GO (RL–GO) hybrid which was prepared by one-step ultrasonication. The results showed that

the removal efficiency of RL–GO is superior to GO when used dosages of adsorbent of 5–15 mg under the experiment conditions. When the pH of the MB solution was increasing from 3 to 11, the amount of dye adsorbed increased from 287.98 to 499.64 mg/g, indicating a strong influence of this parameter on the MB removal with this adsorbent. The adsorption capacity was increased with the increasing temperature, indicating that the adsorption was due to an endothermic process. The main mechanism of adsorption was considered to be the electrostatic interaction between the MB cations, and the negatively charged sites on surface of RL–GO which was corroborated by FTIR spectroscopy. The kinetic data showed an excellent fit to pseudo-second-order model, while the equilibrium data were best fitted to the Freundlich isotherm. The adsorption of MB onto RL–GO was favorable at all temperatures studied.

In their investigation, Madadrang [52] functionalized GO and RGO with N-(trimethoxysilylpropyl) ethylenediamine triacetic acid (EDTA) for use both EDTA-GO and EDTA-RGO as adsorbent on the removal of Pb(II). It was found a good affinity between the Pb(II) ions and EDTA-GO. The adsorption capacity of Pb(II) was increasing of 328 ± 39 mg/g in GO to 479 ± 46 mg/g in EDTA-GO at an equilibrium concentration of 208 ±17 mg/L. EDTA-RGO had a higher surface area (730 m^2/g) respect to GO (430 m^2/g) and EDTA-GO (623 m^2/g); however, their adsorption capacity of Pb(II) was the lowest which was attributed to their low amount of acid groups. The adsorption capacity was dependent of the pH of the solution and the total of acidity groups present in the adsorbent. The adsorption process involved on the removal of Pb(II) with EDTA-GO were the ion-exchange reaction between Pb(II) and –COOH or –OH groups and surface complexation and a complex of Pb(II) with EDTA. The equilibrium data of the adsorption of Pb(II) on EDTA-GO were best fitted to the Langmuir equation. **Figure 4** shows EDTA-GO structure before and after of the interaction with Pb(II) and other heavy metal cations.

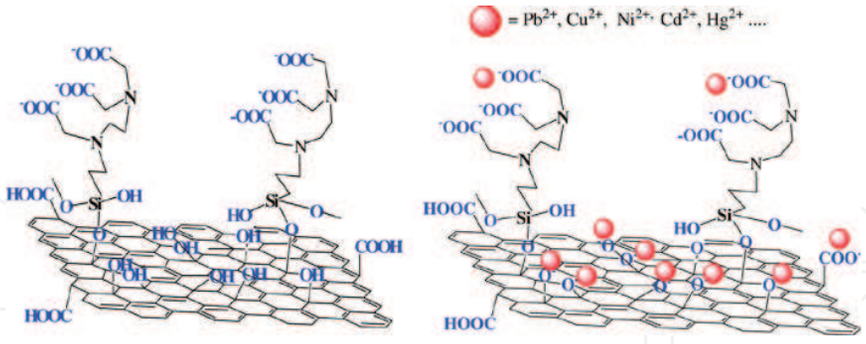

Figure 4. Chemical structure of EDTA-GO before (left) and after of its interaction with heavy metal cations (right). Reprinted with permission from Madadrang et al. [52]. Copyright ©2014, American Chemical Society.

The removal efficiency of Pb(II) using a thiol-functionalized GO (GO-SH) as adsorbent was investigated by Yari [53]. Three different amounts of cysteamine were used as follows 60, 80, and 100 mg which corresponding to GO-SH_1, GO-SH_2, and GO-SH_3 nanocomposites, respectively. The adsorption capacities at equilibrium were 18, 19.8, 20.8, and 21.7 (mg/g) for GO, GO-SH_1, GO-SH_2, and GO-SH_3, respectively. This indicate that the adsorption capacity of Pb(II) onto GO-SHs was increased with the increase in the cysteamine concentration which is due to

a increases in the number of functional groups (S–H) and (N–H) on the adsorbent surfaces. The Pb(II) adsorption increased for all adsorbents with the increase in the pH of the solution from 2 to 7 and when the temperature increased from 288 to 308 K. The results of kinetic experiments suggested that the adsorption of Pb(II) onto the different adsorbents was first due to a surface adsorption and after by possible slow intracellular diffusion in the interior of the adsorbents. On the other hand, the experimental data of equilibrium were well fitted to the Langmuir isotherm model (Type I) for all adsorbents. The negative values of the Gibbs free-energy change of adsorption (ΔG°) and the positive values of enthalpy (ΔH°) indicated that the adsorption process of Pb(II) ion on the GO and GO-SHs were spontaneous and endothermic in nature, respectively.

In another study, Wu [54] prepared a novel adsorbent 3D sulfonated reduced GO (3D-SRGO) aerogel with porous structure, large surface area, excellent hydrophilicity, and high adsorption capacity was prepared, characterized and applied in the Cd(II) ions removal from contaminated water. Filtration experiments revealed that the membranes fabricated by 3D-SRGO could quickly remove Cd(II) ions from the aqueous solutions. Regeneration tests showed that HNO_3 solution can desorb 97.23% cadmium, suggesting that the prepared 3D-SRGO can be repeatedly reused. The SRGO structure shows that there are a number of suspended hydroxyl, carboxylic, and sulfonic groups on the surface; therefore, the adsorption of Cd(II) ions on SRGO is governed by the cation exchange reaction of Cd(II) ions on the SRGO surface. Equilibrium adsorption isotherms are usually used to determine the capacities of adsorbents. The calculated adsorption capacity of the adsorbent for cadmium at pH 6.0 was 234.8 mg/g from Langmuir model, which is higher than many reported adsorbent for cadmium removal.

Li [68] synthesized and used a Chitosan/Sulfydryl-functionalized GO composite (CS/GO-SH) as adsorbent for the adsorption of Pb(II), Cd(II), and Cu(II) in single- and multi-metal ions systems. The adsorption capacities of CS/GO-SH on the individual removal of Pb(II), Cu(II), and Cd(II) were of 447, 425, and 177 mg/g, respectively, at a metal ion concentration of 500 mg/L, pH 5, and 293 K. However, the adsorption capacity of CS/GO-SH for individual metal ion decreased and changed when was used a ternary metal ion system. At each metal ion concentration of 250 mg/L, the adsorption ability of metal ion in mono-component solution followed the order Cu(II) > Pb(II) > Cd(II), while the competitive ability of metal ion in tri-component solution followed the order Cd(II) > Cu(II) > Pb(II). The kinetic experimental data were best fitted to the pseudo-second-order model and the equilibrium experimental data were best fitted to the Freundlich equation for CS/GO-SH. According to the thermodynamic study, the adsorption process of Pb(II), Cu(II), and Cd(II) onto the CS/GO-SH was spontaneous and endothermic.

The elimination of Ni(II) from the aqueous solutions by GO and glycine funcionalized GO (GO-G) was reported by Nafaji [69]. The adsorption capacity of Ni(II) on the two materials increased with the increasing the initial concentration of Ni(II) from 10 to 25 mg/L. The equilibrium data of Ni(II) on GO showed that the adsorption was best fitted of the Langmuir isotherm model (Type II), while the experimental data of the adsorption of Ni(II) on GO-G were best fitted to the Freundlich isotherm model. Both GO and GO-G showed to have a

better adsorption capacity of Ni(II) than some other adsorbents reported in the literature. In this study, the adsorption capacity of Ni(II) by GO-G was only slightly better than the adsorption capacity of GO and this was attributed to the functional groups of the glycine. The removal of Ni(II) by GO decreased when the temperature was increased from 283 to 308 K, while the adsorption of Ni(II) by GO-G decreased until 298 K and after that it was increased. Better results on the removal of Ni(II) were obtained by Wu [61]. In their experimental work, was prepared and used an effective and low-cost porous GO/sawdust composite (GOCC) as adsorbent for the removal of Ni(II) in aqueous solutions. The composite exhibited a strong ability to adsorb nickel ions. The equilibrium data were best fitted to Freundlich isotherm model while the kinetic data showed a better fit to the pseudo-second order kinetic model. The adsorption capacity of Ni(II) was increased considerably from 67.95 mg/g in GO to 98.06 mg/g in GO-G, indicating in this case, that the functionalization of GO improved the removal of Ni(II). This increase in the adsorption capacity of GOCC is attributed to the hydroxyl and carboxyl groups on the GO sheets that increase the ability of the porous GO-G composite to adsorb nickel ions.

As can be seen, GO has a better functionality in the removal of pollutants of water than reduced GO or also called graphene. This difference between GO and reduced GO is attributed to the major amount of oxygenated groups presents on the surface of GO which confer it a hydrophilic character and also interact whit the pollutants as cationic dyes and cationic metal ions. These surface oxygenated groups improve the interaction of GO with other organic molecules with the purpose of to improve the efficiency on the removal of pollutants of water. In general, the functionalization of graphene or GO with other organic molecules improved the adsorption capacity with respect to the individual materials. This increase on the removal of pollutants of water was largely dependent of the acid groups on the surface of GO or reduced GO and present in the organic molecule. Factors as pH of the solution and temperature play an important role on the removal of pollutants with these adsorbents. The removal times of pollutants are very short which indicate that these materials have an important adsorption capacity. The kinetic experimental data of the adsorption of MB and some cationic ions by some functionalized graphene materials showed a well fitted to the pseudo-second-order kinetic model. The equilibrium data of the adsorption of dyes and metal ions on the different functionalized graphene materials were well fitted to the Langmuir and Freundlich isotherm models, but do not showed a tendency by one in special, indicating that the surface homogeneity and heterogeneity of the adsorbents is dependent of the organic molecule nature, the surface of the graphene material and the interaction among them.

3.6. Carbon nanomaterials vs. graphene as adsorbents

As already mentioned above, graphene and GO have demonstrated an important adsorption capacity in the removal of some pollutans of water so they have a promising future in this area. However, these carbonaceous nanomaterials are not the unique that have been used in the decontamination of water. The effectiveness of CNT in the removal of various contaminants of water has been demonstrated in different studies [70–72]. The structural characateristics and electronic properties of graphene, GO, and CNT make them interact with organic

molecules, via non-covalent forces [37]. Furthermore, their nanosized structure also endows them some advantages such as rapid equilibrium rates, high adsorption capacity, and effectiveness over a broad pH range [73]. The exceptional high specific surface area available for adsorption of these nanomaterials makes them will be promising replacement for other adsorbents like AC [74]. Since the emergence of graphene in 2004, comparisons between graphene and CNT for different applications have been investigated.

Despite of be carbonaceous materials, graphene and CNT have different topology. Graphene is the hypothetical infinite aromatic sheet with sp^2 hybridization of the carbon atoms [75]. On the other hand, the structure of MWCNT can be rationalized as resulting from the folding of several graphene sheets (sp^2-hybridized carbon) aligned in a concentric manner [76]. This topological variation can result in different interactions between the carbon adsorbent and the contaminant molecule which has direct influence in the adsorption capacity [29]. Besides topology, the content of surface oxygenated groups play an important role on the adsorption capacity of CNM. Some investigations have compared the performance of graphene and CNT as adsorbents of pollutants molecules present in aqueous solutions at the same conditions in order to determinate which nanomaterial is more efficient in the decontamination of water by adsorption.

The removal of methylene blue by GO and CNT was reported by Li [37]. Both nanomaterials were modified by nitric acid. The surface oxygenated groups were identified by infrared spectroscopy. The removal efficiencies reached were 94.8–98.8% for GO and 72.4–82.7% for CNT in the pH range from 2 to 9, where both nanomaterials showed be negatively charged which enhanced the adsorption of the positively charged MB. The adsorption capacities for GO and CNT were 240.65 and 176.02 mg/g, respectively, at initial concentration of 120 mg/L. The experimental adsorption data for both nanomaterials were well fitted to the Langmuir equation model. The kinetic study of the adsorption of MB onto GO and CNT showed that the experimental data were best fitted to the pseudo-second-order kinetic model. The initial adsorption stage of GO is faster than CNT. This was attributed to the single-atom-layered structure of GO which benefited the attraction of dye molecules speedy. The highest normalized adsorption capacity of GO was due to the largest surface area accessibility which was attributed to its unique single-atom-layered structure. Electron donor acceptor interactions, π–π electron coupling and electrostatic interactions are the mechanisms that favored the adsorption of MB onto GO and CNT.

Elsagh [46] investigated the elimination of cationic dye Basic Red 46 (BR46) from aqueous solutions using as adsorbents GO, graphene, single-walled CNT (SWCNT), carboxylate group functionalized SWCNT (SWCNT-COOH). The adsorption kinetic data of GE and GO were well fitted to the pseudo-second-order model, while the experimental data of SWCNT and SWCTN-COOH were best fitted to the pseudo-first-order model. The adsorption capacity order of the different CNM used was SWCNT-COOH > SWCNT > GO > GE. The adsorption capacity was increased with increasing of the initial dye concentration and with increasing the pH of the dye solution and reached a maximum level at the pH of 9. The equilibrium experimental data of adsorption of BR46 on the four adsorbents were well fitted to the Langmuir

equation model. The physisorption was found to be the main adsorption mechanism and the rate-limiting step was mainly surface adsorption.

The adsorption of reactive red 2 (RR2) using RGO, GO, MWCNT, and oxidized multiwalled CNT (O-MWCNT) was investigated by Pérez-Ramírez [77]. The influence of the dosage of adsorbent and the dimension of the CNM on the removal of RR2 was studied. The adsorption of RR2 increased with increasing the loading of adsorbent. The better performance on the removal of RR2 was reached by MWCNT and O-MWCNT, which removed almost the total color of the solution. The order of the adsorption of RR2 was MWCNT = O-MWCNT > GO > RGO at adsorbent loading of 0.75 g/L. The effect of the contact time can be seen in **Figure 5**. Factors such as surface area, surface-oxygenated groups, the shape of the carbon structures, and the nature of the dye played an important role in this adsorption process. The main adsorption mechanism for the removal of RR2 was via π–π interactions between the aromatic rings. The kinetic adsorption data were better fitted to the pseudo-second-order model. The results suggested that the RR2 adsorption onto RGO, GO, MWCNT, and O-MWCNT was through a physisorption process but with strong interactions. The removal of RR2 was strongly influenced by the dimension of the CNM. One dimension of MWCNT and O-MWCNT allow them to have an arrangement (entangled) which produce different available sites for adsorption [78] unlike of 2D nanomaterials as RGO and GO where the available sites for adsorption are found on the external surface and maybe in the interplanar space.

The Cu(II) removal from aqueous solutions by GO and CNT was studied and reported by Ren [29]. Infrared spectroscopy showed the presence of oxygen-containing functional groups on the surface of all carbon materials, which provide chemical adsorption sites for heavy metal ions. The effect of pH and Cu(II) initial concentration were investigated. At the low acidic pH medium, the oxygenated groups on the surface of the GO and MWCNT were positively

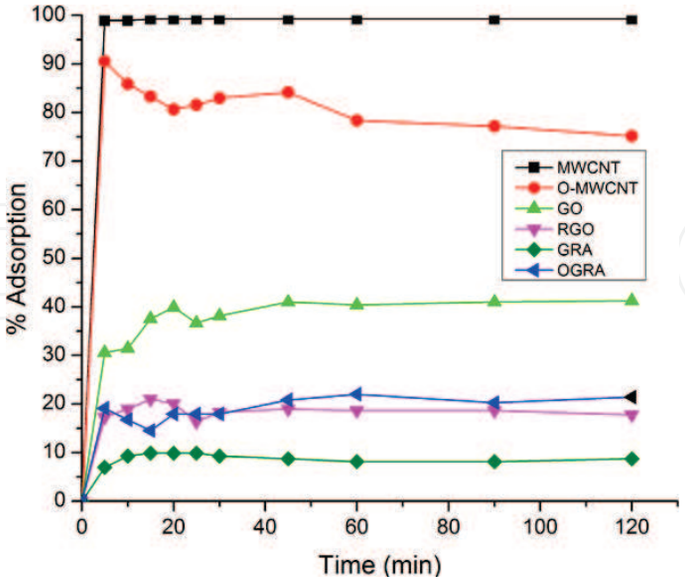

Figure 5. Effect of contact time on removal of RR2 by MWCNT, O-MWCNT, GO, RGO, graphite (GRA), and graphite oxide (OGRA). Adapted with permission from Pérez-Ramírez et al. [77]. Copyright ©2015, Mary Ann Liebert, Inc.

charged generating electrostatic repulsion with the free metal ions which leaded to a low adsorption percentage. At alkaline pH medium, these oxygenated groups were negatively charged generating attraction for the free metal ions and metal ions can form precipitates as their hydroxides. Therefore, the increase in the adsorption at alkaline pH was attributed to the electrostatic attraction, inner-sphere surface complexation, and surface precipitation. At pH range from 7 to 10, the adsorption percentage of Cu by GO and MWCNT was very similar; however, at pH 5, the adsorption percentage obtained by GO was around of 75%, while for MWCNT was minor to 20%. The adsorption experimental data were better fitted to Langmuir model. The maximum adsorption capacities of Cu(II) according to Langmuir were 1.18×10^{-3} and 3.19×10^{-5} mol g^{-1} for GO and MWCNT, respectively. The more important factors controlling the adsorption of Cu(II) on GO and MWCNT were the speciation in solution and adsorbate–adsorbent interaction across all the pH values.

Smith [79] investigated the removal of Lisozyme protein in water by graphene, GO, and SWCNT. Protein adsorption capacity of the CNM was evaluated to different initial concentrations of Lisozyme in aqueous solutions. The capacities adsorption order were GO > SWCNT > GE. GO exhibited an adsorption capacity of 500 mg/g with an initial Lysozyme concentration of 0.4 mg/mL, while SWCNT and GE obtained an adsorption capacity minor to 100 mg/g at the same conditions. The abundance of carboxylic acid groups on the surface of GO can cause an attractive electrostatic force with the positively charged Lisozyme being the cause of the high adsorption performance of this nanomaterial. Furthermore, the hydrophilic character of GO could facilitate the interaction with the protein. The adsorption of the Lisozyme onto SWNT and GE could be attributed to the van der Waals forces and some electrostatic interactions. In the equilibrium study, the nanomaterial with the highest adsorption capacity at all initial concentration was GO. The Langmuir, Freundlich, and Temkin models were used to model the adsorption experimental data of the protein onto GO, GE, and SWCNT. The adsorption data of Lysozyme onto SWCNT and GE were better fitted to the Langmuir equation model ($R^2 = 0.94$ and 0.98, respectively), while the values of R^2 in Langmuir, Freundlich, and Temkin models for GO were 0.656, 0.616, and 0.741, respectively. However, the high value of adsorption capacity of GO in Langmuir model (1428.57 mg/g) indicated a high adsorption. Further, the high value of K_T (198.97) suggested the electrostatic interactions as possible mechanism of the Lysosyme protein adsorption onto GO. According to results, GO, GE, and SWCNT were more efficient on the removal of organic fouling agents than AC.

Adsorption of phenanthrene (PNT) and biphenyl (BP) by graphene nanosheets A and B (GNS-A and GNS-B), GO, SWCNT and MWCNT was investigated by Apul [80]. Phenanthrene and biphenyl solutions were prepared with distilled and deionized water and in the presence of natural organic matter (NOM). The surface area of the different CNM was GNS-A >GO > GNS-B > SWCNT > MWCNT. Adsorption capacities for PNT in distillate and deionized water at C_e = 1 mg/L were higher than BP for all adsorbent nanomaterials. The order of the adsorption capacities of PNT was SWCNT > GNS-A > GNS-B ~ GO > MWCNT, while the order for BP adsorption capacities was SWCNT > GNS-A ~ GNS-B > GO > MWCNT. The adsorption was depending on the surface area, pore size, and oxygen content of CNM as well as hydropho-

bicity and molecular structure of adsorbates. The adsorption capacities of PNT and BP under NOM preloading followed a similar order than the obtained in distillate and deionized water but it decreased. The influence of NOM on the PNT and BP adsorption was smaller on GNS-A and GNS-B than SWCNT and MWCNT which was attributed to a lower compact bundle structure for graphenes than SWCNT or MWCNT aggregates.

A comparative study on removal of phenol with respect to the dimension of the nanomaterial (1D and 2D nanomaterials in their unoxidized and oxidized forms) was carried out by de la Luz-Asunción [45]. Six adsorbents such as SWCNT, MWCNT, oxidized SWCNT (O-SWCNT), O-MWCNT, GO, and RGO were employed. The adsorption kinetics indicate that most of phenol removal takes place during the first 50 min. It is implied that CNM possess very strong adsorption ability for phenol. The pseudo-second-order model provides the best correlation for the adsorption data ($R^2 > 0.99$). The results indicate that Freundlich isotherm provides the best fit for the equilibrium data ($R^2 > 0.94$). Differences in adsorption capacity between 1D and 2D nanomaterials are shown by the parameter, K_F, obtained from Freundlich isotherm. K_F, decreases in the following order: GO (7.456) > MWCNT (6.162) > O-MWCNT (4.777) > RGO (4.338). R_L values are between 0 and 1; this represents favorable adsorption between CNM and phenol. The adsorption process occurs by hydrogen bonding (**Figure 6**a) and mainly by π–π interactions (**Figure 6**b) and not by electrostatic interactions. The mechanism of interaction between RGO and GO with phenol is similar to CNT and OCNT.

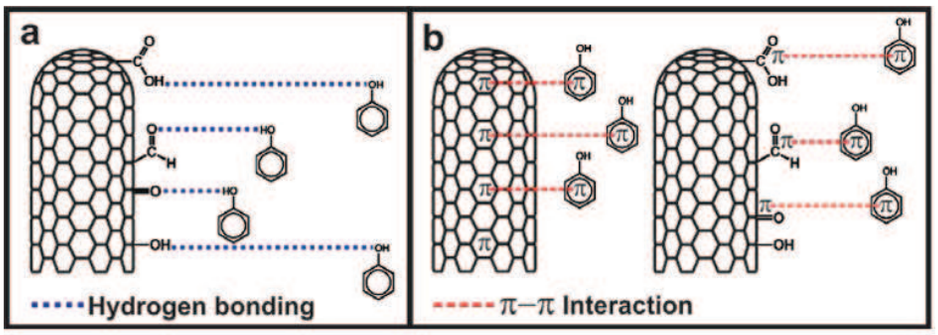

Figure 6. Proposed mechanisms of interaction between carbon nanotubes in their unoxidized and oxidized forms with phenol. Reprinted with permission from de la Luz-Asunción et al. [45]copyright 2015 Hindawi Publishing Corporation.

In an interesting study, Balamurugan [81] investigated the adsorption of chlorobenzenes (CBs) onto (5, 5) armchair SWCNT and graphene sheet through of density functional theory-based calculations. The interaction between the SWCNT and GE with CBs was studied with the Bader's theory of atoms. The interaction energy of the CBs increased according to the chlorine content was increasing from one to six atoms for both SWCNT and GE. The values of interaction energy were higher for G-CBs than those of SWCNT-CBs, and the variation of the interaction energy between both systems was found in the range from 2.30 to 3.42 Kcal/mol. On the other hand, GE presented a better adsorption capacity of CBs than SWCNT. This was attributed to the planar geometry of graphene which facilities the adsorption surface of pollutants. With the increasing of the chlorine content, the solubility of the CBs decreased while

their toxicity increased. The electrostatic interactions play an important role in the adsorption process of CBs onto SWCNT and GE. A summary with the different systems of adsorption and the kinetic models and Isotherms which were best fitted to the adsorption data are found in **Table 5**.

Adsorbent	Adsorbate	Kinetic model	Isotherm	References
GO	MB	Pseudo-second-order	Langmuir	[37]
CNTs	MB	Pseudo-second-order	Langmuir	[37]
GO	BR46	Pseudo-second-order	Langmuir	[46]
G	BR46	Pseudo-second order	Langmuir	[46]
SWCNT	BR46	Pseudo-first order	Langmuir	[46]
SWCNT-COOH	BR46	Pseudo-first order	Langmuir	[46]
GO	RR2	Pseudo-first order		[77]
rGO	RR2	Pseudo-first order		[77]
MWCNT	RR2	Pseudo-first order		[77]
OMWCNT	RR2	Pseudo-first order		[77]
G	PNT		Freundlich	[80]
G	PNT		Freundlich	[80]
GO	PNT		Freundlich	[80]
SWCNT	PNT		Freundlich	[80]
MWCNT	PNT		Freundlich	[80]
G	BP		Freundlich	[80]
G	BP		Freundlich	[80]
GO	BP		Freundlich	[80]
SWCNT	BP		Freundlich	[80]
MWCNT	BP		Freundlich	[80]
GO	Cu(II)		Langmuir	[29]
MWCNT	Cu(II)		Langmuir	[29]
G	Lysozime		Langmuir	[79]
GO	Lysozime		Temkin	[79]
SWNT	Lysozime		Langmuir	[79]

BP, biphenyl; BR 46, basic red 46; Cu, copper; MB, methylene blue; PNT, phenanthrene ; RR2, reactive red 2..

Table 5. Adsorption results of different pollutants from water onto carbon nanomaterials.

It is difficult to say whether graphene is better than CNT or vice versa. Results of the different investigations where these nanomaterials were compared indicated that there are some factors such as surface area, surface oxygenated groups, and pH solution which have strong influence on the adsorption of pollutants in water onto graphene and CNT. In both materials, the equilibrium adsorption time is short. The planar and tubular structure of graphene and CNT, respectively, and the contaminant molecule structure play an important role on the adsorption process and therefore the efficiency of this.

4. Concluding remarks

The results of graphene materials and graphene-based materials in photocatalysis and adsorption indicate that these materials have a great future in the decontamination of water. GO has shown photocatalytic activity when has been used of individual form on the removal of contaminants from water. Besides, the combination of graphene materials with different semiconductor nanoparticles has shown good results on the removal pollutans, increasing the efficiency of the photocatalytic process due to a charge separation more efficient. On the other hand, the removal of pollutant from water by adsorption using graphene materials as adsorbents shows a favorable panorama. The efficiency of these materials on the removal of heavy metals and organic compounds from water will be depending on factors such as surface area, pH, temperature, surface charge, content of functional groups, among others. Surface oxygenated groups in the graphene sheets improve the interaction with cationic dyes and cationic metal ions. The functionalization of graphene with different functional groups can be used to obtain a better affinity for the contaminant, thus improving the efficiency of adsorption process. Definitely, graphene materials are promising to play an important role in the photocatalysis and adsorption processes for environmental remediation.

Author details

Eduardo E. Pérez-Ramírez, Miguel de la Luz-Asunción, Ana L. Martínez-Hernández and Carlos Velasco-Santos*

*Address all correspondence to: cylaura@gmail.com

Division of Graduate Studies and Research, The Technological Institute of Querétaro, Santiago de Querétaro, Querétaro, México

References

[1] Nguyen-Phan T-D, Pham VH, Shin EW, Pham H-D, Kim S, Chung J S, Kim EJ, Hur S H. The role of graphene oxide content on the adsorption-enhanced photocatalysis of titanium dioxide/graphene oxide composites. Chemical Engineering Journal. 2011; 170:226–232. doi:10.1016/j.cej.2011.03.060

[2] Min Y, Zhang K, Zhao W, Zheng F, Chen Y, Zhang Y. Enhanced chemical interaction between TiO_2 and graphene oxide for photocatalytic decolorization of methylene blue. Chemical Engineering Journal. 2012; 193–194:203–210. doi:10.1016/j.cej.2012.04.047

[3] Rong X, Qiu F, Zhang C, Fu L, Wang Y, Yang D. Preparation, characterization and photocatalytic application of TiO_2–graphene photocatalyst under visible light irradiation. Ceramics International. 2014; 41:2502–2511. doi:10.1016/j.ceramint.2014.10.072

[4] Gao P, Li A, Sun D D, Ng W. Effects of various TiO_2 nanostructures and graphene oxide on photocatalytic activity of TiO_2. Journal of Hazardous Materials. 2014; 279:96–104. doi:10.1016/j.jhazmat.2014.06.061

[5] Han F, Li F, Yang J, Cai X, Fu L. One-pot synthesis of coprous oxide-reduced graphene oxide nanocomposite wit enhanced photocatalytic and electrocatalytic performance. Physica E: Low Dimensional Systems and Nanostructures. 2016; 77:122–126. doi:10.1016/j.physe.2015.11.020

[6] Zhigang N. Reduced graphene oxide-cuprous oxide hybrid nanopowders: Hydrothermal synthesis and enhanced photocatalytic performance under visible light irradiation. Materials Science in Semiconductor Processing. 2014; 23:78–84. doi:10.1016/j.mssp.2014.02.026

[7] Sun L, Wang G, Hao R, Han D, Cao S. Solvothermal fabrication and enhanced visible light photocatalytic activity of Cu_2O-reduced graphene oxide composite microspheres for photodegradation of rhodamine B. Applied Surface Science. 2015; 358:91–99. doi:10.1016/j.apsusc.2015.08.128

[8] Zou W, Zhang L, Liu L, Wang X, Sun J, Wu S, Deng Y, Tang C, Gao F, Dong L. Engineering the Cu_2-reduced graphene oxide interface to enhance photocatalytic degradation of organic pollutants under visible light. Applied Catalysis B, Environmental. 2015; 181:495–503. doi:10.1016/j.apcatb.2015.08.017

[9] Tayyebi A, Outokesh M, Tayebi M, Shafikhani A, Şengör S S. ZnO quantum dots-graphene composites: Formation mechanism and enhanced photocatalytic activity for degradation of methyl orange dye. Journal of Alloys and Compound. 2016; 663:738–749. doi:10.1016/j.jallcom.2015.12.169.

[10] Rabieh S, Nassimi K, Bagheri M. Synthesis of hierarchical ZnO-reduced graphene oxide nanocomposites with enhanced adsorption-photocatalytic performance. Materials Letters. 2016; 162:28–31. doi:10.1016/j.matlet.2015.09.111

[11] Huang K, Li Y H, Lin S, Liang C, Wang H, Ye C X, Wang Y J, Zhang R, Fan D Y, Yang H J, Wang Y G, Lei M. A facile route to reduced graphene oxide–zinc oxide nanorod composites with enhanced photocatalytic activity. Powder Technology. 2014; 257:113–119. doi:10.1016/j.powtec.2014.02.047

[12] Zhang C, Zhang J, Su Y, Xu M, Yang Z, Zhang Y. ZnO nanowire/reduced graphene oxide nanocomposites for significantly enhanced photocatalytic degradation of Rhodamine 6G. Physica E. 2014; 56:251–255. doi:10.1016/j.physe.2013.09.020

[13] Upadhyay R K, Soin N, Roy S S. Role of graphene/metal oxide composites as photocatalysts, adsorbents and disinfectants in water treatment: A review. RSC Advances. 2014; 4: 3823–3851. doi:10.1039/c3ra45013a

[14] Chakraborty K, Chakrabarty S, Das P, Ghosh S, Pal T. UV-assisted synthesis of reduced graphene oxide zinc sulfide composite with enhanced photocatalytic activity. Materials Science and Engineering B. 2016; 204:8–14. doi:10.1016/j.mseb.2015.11.001

[15] Zou L, Wang X, Xu X, Wang H. Reduced graphene oxide wrapped CdS composites with enhanced photocatalytic performance and high stability. Ceramics International. 2016; 42:372–378. doi:10.1016/j.ceramint.2015.08.119

[16] Raghavan N, Thangavel S, Venugopal G. Enhanced photocatalytic degradation of methylene blue by reduced graphene-oxide/titanium dioxide/zinc oxide ternary nanocomposites. Materials Science in Semiconductor Processing. 2015; 30:321–329. doi:10.1016/j.mssp.2014.09.019

[17] Almeida B M, Jr Melo A M, Bettini J, Benedetti J E, Nogueira A F. A novel nanocomposite based on TiO_2/Cu_2O/reduced graphene oxide with enhanced solar-light-driven photocatalytic activity. Applied Surface Science. 2015; 324:419–431. doi:10.1016/j.apsusc.2014.10.105

[18] Li J, Wei L, Yu C, Fang W, Xie Y, Zhou W, Zhu L. Preparation and characterization of graphene oxide/Ag_2CO_3 photocatalyst and its visible light photocatalytic activity. Applied Surface Science. 2015; 358:168–174. doi:10.1016/j.apsusc.2015.07.007

[19] Wang C, Zhu J, Wu X, Xu H, Song Y, Yan J, Song Y, Ji H, Wang K, Li H. Photocatalytic degradation of bisphenol A and dye by graphene-oxide/ Ag_3PO_4 composite under visible light irradiation. Ceramics International. 2014; 40:8061–8070. doi:10.1016/j.ceramint.2013.12.159

[20] Chen X-J, Dai Y-Z, Wang X-Y, Guo J, Liu T-H, Li F-F. Synthesis and characterization of Ag_3PO_4 immobilized with graphene oxide (GO) for enhanced photocatalytic activity and stability over 2,4-dichlorophenol under visible light irradiation. Journal of Hazardous Materials. 2015; 292:9–18. doi:10.1016/j.jhazmat.2015.01.032

[21] Zhang Y, Shen B, Huang H, He Y, Fei B, Lv F. $BiPO_4$/reduced graphene oxide composites photocatalyst with highphotocatalytic activity. Applied Surface Science. 2014; 319:272–277. doi:10.1016/j.apsusc.2014.07.052

[22] Hsu H-C, Shown I, Wei H-Y, Chang Y-C, Du H-Y, Lin Y-G, Tseng C-A, Wang C-H, Chen L-C, Lin Y-C, Chen K-H. Graphene oxide as a promising photocatalyst for CO_2 to methanol conversion. Nanoscale. 2013; 5:262–268. doi:10.1039/c2nr31718d

[23] Yeh T-F, Syu J-M, Cheng C, Chang T-H, Teng H. Graphite oxide as a photocatalyst for hydrogen production from water. Advanced Functional Materials. 2010; 20:2255–2262. doi:10.1002/adfm.201000274

[24] Krishnamoorthy K, Mohan R, Kim S-J. Graphene oxide as a fotocatalytic material. Applied Physics Letters. 2011; 98:244101 (1–3). doi:10.1063/1.3599453

[25] Bustos-Ramirez K, Barrera-Diaz CE, De Icaza M, Martínez-Hernández AL, Velasco-Santos C. Photocatalytic activity in phenol removal of water from graphite and graphene oxides: Effect of degassing and chemical oxidation in the synthesis process. Journal of Chemistry. 2015; 2015; 1–10. doi:10.1155/2015/254631

[26] Bustos-Ramirez K, Barrera-Diaz C E, De Icaza M, Martínez-Hernández A L, Velasco-Santos C. 4-chlorophenol removal from water using graphite and graphene oxides as photocatalysts. Journal of Environmental Health Science & Engineering. 2015; 13. 1-10. doi:10.1186/s40201-015-0184-0.

[27] Kim H, Kang S O, Park S, Park H S. Adsorption isotherms and kinetics of cationic and anionic dyes on three-dimensional reduced graphene oxide macrostructure. Journal of Industrial and Engineering Chemistry. 2015; 21:1191–1196. doi:10.1016/j.jiec.2014.05.033.

[28] Moradi O, Gupta V K, Agarwal S, Tyagi I, Asif M, Makhlouf A S H, et al. Characteristics and electrical conductivity of graphene and graphene oxide for adsorption of cationic dyes from liquids: Kinetic and thermodynamic study. Journal of Industrial and Engineering Chemistry. 2015; 28:294–301. doi:10.1016/j.jiec.2015.03.005.

[29] Ren X, Li J, Tan X, Wang X. Comparative study of graphene oxide, activated carbon and carbon nanotubes as adsorbents for copper decontamination. Dalton Transactions. 2013; 42(15):5266–5274. doi:10.1039/c3dt32969k.

[30] Yang S-T, Chen S, Chang Y, Cao A, Liu Y, Wang H. Removal of methylene blue from aqueous solution by graphene oxide. Journal of Colloid and Interface Science. 2011; 359:24–29. doi:10.1016/j.jcis.2011.02.064.

[31] Fan L, Luo C, Sun M, Qiu H, Li X. Synthesis of magnetic β-cyclodextrin-chitosan/graphene oxide as nanoadsorbent and its application in dye adsorption and removal. Colloids Surfaces B Biointerfaces. 2013; 103:601–607. doi:10.1016/j.colsurfb.2012.11.023.

[32] Li Y H, Di Z, Ding J, Wu D, Luan Z, Zhu Y. Adsorption thermodynamic, kinetic and desorption studies of Pb2+ on carbon nanotubes. Water Research. 2005; 39(4):605–609. doi:10.1016/j.watres.2004.11.004.

[33] Kabbashi N A, Atieh M A, Al-Mamun A, Mirghami M E, Alam M D Z, Yahya N. Kinetic adsorption of application of carbon nanotubes for Pb(II) removal from aqueous

solution. Journal of Environmental Sciences. 2009; 21(4):539–544. doi:10.1016/s1001-0742(08)62305-0.

[34] Sun L, Yu H, Fugetsu B. Graphene oxide adsorption enhanced by in situ reduction with sodium hydrosulfite to remove acridine orange from aqueous solution. Journal of Hazardous Materials. 2012; 203–204:101–110. doi:10.1016/j.jhazmat.2011.11.097.

[35] Wang F, Haftka J J H, Sinnige T L, Hermens J L M, Chen W. Adsorption of polar, nonpolar, and substituted aromatics to colloidal graphene oxide nanoparticles. Environmental Pollution. 2014; 186:226–233. doi:10.1016/j.envpol.2013.12.010.

[36] Ramesha G K, Vijaya Kumara A, Muralidhara H B, Sampath S. Graphene and graphene oxide as effective adsorbents toward anionic and cationic dyes. Journal of Colloid Interface Science. 2011; 361(1):270–277. doi:10.1016/j.jcis.2011.05.050.

[37] Li Y, Du Q, Liu T, Peng X, Wang J, Sun J. Comparative study of methylene blue dye adsorption onto activated carbon, graphene oxide, and carbon nanotubes. Chemical Engineering Research and Design. 2013; 91(2):361–368. doi:10.1016/j.cherd.2012.07.007.

[38] Wang H J, Zhou A L, Peng F, Yu H, Chen LF. Adsorption characteristic of acidified carbon nanotubes for heavy metal Pb(II) in aqueous solution. Materials Science and Engineering A. 2007; 466(1–2):201–206. doi:10.1016/j.msea.2007.02.097.

[39] Zhang W, Zhou C, Zhou W, Lei A, Zhang Q, Wan Q. Fast and considerable adsorption of methylene blue dye onto graphene oxide. Bulletin of Environmental Contamination and Toxicology. 2011; 87(1):86–90. doi:10.1007/s00128-011-0304-1.

[40] Liu T, Li Y, Du Q, Sun J, Jiao Y, Yang G. Adsorption of methylene blue from aqueous solution by graphene. Colloids Surfaces B Biointerfaces. 2012; 90(1):197–203. doi:10.1016/j.colsurfb.2011.10.019.

[41] Arasteh R, Masoumi M, Rashidi A M, Moradi L, Samimi V, Mostafavi S T. Adsorption of 2-nitrophenol by multi-wall carbon nanotubes from aqueous solutions. Applied Surface Science. 2010; 256(14):4447–4455. doi:10.1016/j.apsusc.2010.01.057.

[42] Zhao G, Li J, Wang X. Kinetic and thermodynamic study of 1-naphthol adsorption from aqueous solution to sulfonated graphene nanosheets. Chemical Engineering Journal. 2011; 173(1):185–190. doi:10.1016/j.cej.2011.07.072.

[43] Kuo CY. Comparison with as-grown and microwave modified carbon nanotubes to removal aqueous bisphenol A. Desalination. 2009; 249(3):976–982. doi:10.1016/j.desal.2009.06.058.

[44] Hu X-J, Liu Y-G, Wang H, Zeng G-M, Hu X, Guo Y-M, Li T-T, Chen A-W, Jiang L-H, Guo F-Y. Adsorption of copper by magnetic graphene oxide-supported β-cyclodextrin: Effects of pH, ionic strength, background electrolytes, and citric acid. Chemical Engineering Research and Design. 2015; 93: 675–683. doi:10.1016/j.cherd.2014.06.002

[45] de la Luz-Asunción M, Sánchez-Mendieta V, Martínez-Hernández A L, Castaño, V M, Velasco-Santos C. Adsorption of phenol from aqueous solutions by carbon nanomate-

rials of one and two dimensions: Kinetic and equilibrium studies. Journal of Nanomaterials. 2015; 2015:1–15. doi:10.1155/2015/405036.

[46] Elsagh A, Moradi O, Fakhri A, Najafi F, Alizadeh R, Haddadi V. Evaluation of the potential cationic dye removal using adsorption by graphene and carbon nanotubes as adsorbents surfaces. Arabian Journal of Chemistry. 2014; 1–8 doi:10.1016/j.arabjc.2013.11.013.

[47] Yu X, Luo T, Zhang Y, Jia Y, Zhu B, Fu X. Adsorption of Lead (II) on O_2-plasma-oxidized multiwalled carbon nanotubes®: Thermodynamics , kinetics , and desorption. Applied Materials and Interfaces. 2011; 3(7):2585–2593. doi:10.1021/am2004202.

[48] Ahmaruzzaman M. Industrial wastes as low-cost potential adsorbents for the treatment of wastewater laden with heavy metals. Advances in Colloid and Interface Science. 2011; 166(1–2):36–59. doi:10.1016/j.cis.2011.04.005.

[49] Wang H, Yuan X, Wu Y, Huang H, Zeng G, Liu Y. Adsorption characteristics and behaviors of graphene oxide for Zn(II) removal from aqueous solution. Applied Surface Science. 2013; 279:432–440. doi:10.1016/j.apsusc.2013.04.133.

[50] Tan P, Sun J, Hu Y, Fang Z, Bi Q, Chen Y. Adsorption of Cu2+, Cd2+ and Ni2+ from aqueous single metal solutions on graphene oxide membranes. Journal of Hazardous Materials. 2015; 297:251–260. doi:10.1016/j.jhazmat.2015.04.068.

[51] Yang S, Li L, Pei Z, Li C, Lv J, Xie J. Adsorption kinetics, isotherms and thermodynamics of Cr(III) on graphene oxide. Colloids and Surfaces A: Physicochemical and Engineering Aspects. 2014; 457(1):100-106. doi:10.1016/j.colsurfa.2014.05.062.

[52] Madadrang C J, Kim H Y, Gao G, Wang N, Zhu J, Feng H. Adsorption behavior of EDTA-graphene oxide for Pb(II) removal. ACS Applied Materials and Interfaces. 2012; 4(3):1186-1193. doi:10.1021/am201645g.

[53] Yari M, Norouzi M, Mahvi A H, Rajabi M, Yari A, Moradi O. Removal of Pb(II) ion from aqueous solution by graphene oxide and functionalized graphene oxide-thiol: Effect of cysteamine concentration on the bonding constant. Desalination and Water Treatment. 2015; 1-16. doi:10.1080/19443994.2015.1043953.

[54] Wu S, Zhang K, Wang X, Jia Y, Sun B, Luo T, Meng F, Jin Z, Lin D, Shen W, Kong L, Liu J. Enhanced adsorption of cadmium ions by 3D sulfonated reduced graphene oxide. Chemical Engineering Journal. 2015; 57. 262:1292-1302. doi:10.1016/j.cej.2014.10.092.

[55] Li Y, Du Q, Liu T, Sun J, Jiao Y, Xia Y. Equilibrium, kinetic and thermodynamic studies on the adsorption of phenol onto graphene. Materials Research Bulletin. 2012; 47(8): 1898–1904. doi:10.1016/j.materresbull.2012.04.021.

[56] Ahmed S, Rasul M G, Martens W N, Brown R J, Hashib M A. Heterogeneous photocatalytic degradation of phenols in waste water: A review on current status and developments. Desalination. 2010; 261(1–2):3–18. doi:10.1016/j.desal.2010.04.062.

[57] Yan H, Tao X, Yang Z, Li K, Yang H, Li A. Effects of the oxidation degree on the adsorption of methylene blue. Journal of Hazardous Materials. 2014; 268:191–198. doi: 10.1016/j.jhazmat.2014.01.015.

[58] Mehrizad A, Gharbani P. Decontamination of 4-chloro-2-nitrophenol from aqueous solution by graphene adsorption: Equilibrium, kinetic, and thermodynamic studies. Polish Journal of Environmental Studies. 2014; 23(6):2111–2116. doi:10.15244/pjoes/26779.

[59] Pavagadhi S, Tang A L L, Sathishkumar M, Loh K P, Balasubramanian R. Removal of microcystin-LR and microcystin-RR by graphene oxide: Adsorption and kinetic experiments. Water Research. 2013; 47(13):4621–4629. doi:10.1016/j.watres.2013.04.033.

[60] Nam S-W, Jung C, Li H, Yu M, Flora J R V, Boateng L K. Adsorption characteristics of diclofenac and sulfamethoxazole to graphene oxide in aqueous solution. Chemosphere. 2015; 136:20–26. doi:10.1016/j.chemosphere.2015.03.061.

[61] Wu Z, Zhong H, Yuan X, Wang H, Wang L, Chen X, Zeng G, Wu Y. Adsorptive removal of methylene blue by rhamnolipid-functionalized graphene oxide from wastewater. Water Research. 2014; 67:330–344. doi:10.1016/j.watres.2014.09.026

[62] Bianco A. Graphene: safe or toxic? The two faces of the medal. Angewandte Chemie International Edition. 2013; 52:4986–4997. doi:10.1002/anie.201209099

[63] Chen L, Hu P, Zhang L, Huang S, Luo L, Huang C. Toxicity of graphene oxide and multi-walled carbon nanotubes against human cells and zebrafish. Science China Chemistry. 2012; 55:2209–2216. doi:10.1007/s11426-012-4620-z

[64] Kuilla T, Bhadrab S, Yaoa D, Hoon Kimc N, Bosed S, HeeLee J. Recent advances in graphene based polymer composites. Progress in Polymer Science. 2010; 35:1350–1375. doi:10.1016/j.progpolymsci.2010.07.005

[65] Anirudhan T, Sreekumari S. Adsorptive removal of heavy metal ions from industrial effluents using activated carbon derived from waste coconut buttons. Journal of Environmental Sciences. 2011; 23:1989–1998. doi:10.1016/s1001-0742(10)60515–3

[66] Zhao M, Liu P. Adsorption of methylene blue from aqueous solutions by modified expanded graphite powder. Desalination. 2009; 249:331–336. doi:10.1016/j.desal.2009.01.037

[67] Aguado J, Arsuaga J M, Arencibia A, Lindo M, Gascón V. Aqueous heavy metals removal by adsorption on amine-functionalized mesoporous silica. Journal of Hazardous Materials. 2009; 163:213–221. doi:10.1016/j.jhazmat.2008.06.080

[68] Li X, Zhou H, Wu W, Wei S, Xu Y, Kuang Y. Studies of heavy metal ion adsorption on Chitosan/Sulfydryl functionalized graphene oxide composites. Journal of Colloid and Interface Science. 2015; 448:389–397. doi:10.1016/j.jcis.2015.02.039

[69] Najafi F, Moradi O, Rajabi M, Asif M, Tyagi I. Agarwa S, Gupta V K. Thermodynamics of the adsorption of nickel ions from aqueous phase using graphene oxide and

glycine functionalized graphene oxide. Journal of Molecular Liquids. 2015; 208:106–113. doi:10.1016/j.molliq.2015.04.033

[70] Prola LDT, Machado FM, Bergmann CP, de Souza FE, Gally CR, Lima E C, Adebayo MA, Dias SLP, Calvete T. Adsorption of Direct Blue 53 dye from aqueous solutions by multi-walled carbon nanotubes and activated carbon. Journal of Environmental Management. 2013; 130:166–175. doi:10.1016/j.jenvman.2013.09.003

[71] Xu D, Tan X, Chen C, Wang X. Removal of Pb(II) from aqueous solution by oxidized multiwalled carbon nanotubes. Journal of Hazardous Materials. 2008; 154:407–416. doi:10.1016/j.jhazmat.2007.10.059

[72] Kragulj M, Trickovic J, Kukovecz A, Jovic B, Molnar J, Roncevic S, Kónya Z, Dalmacija B. Adsorption of chlorinated phenols on multiwalled carbon nanotubes. Royal Society of Chemistry Advances. 2015; 5, 24920–24929. doi:10.1039/c5ra03395k

[73] Mauter M S, Elimelech M. Environmental applications of carbon-based nanomaterials. Environmental Science Technology. 2008; 42:5843–5859. doi:10.1021/es8006904

[74] Zhang X, Cheng C, Zhao J, Ma L, Sun S, Zhao C. Polyethersulfone enwrapped graphene oxide porous particles for water treatment. Chemical Engineering Journal. 2013; 215–216:72–81. doi:10.1016/J.CEJ.2012.11.009

[75] Niyogi S, Bekyarova E, Itkis M E, Mc Williams J L, Hamon M A, Haddon R C. Solution properties of graphite and graphene. Journal American Chemical Society. 2006; 128:7720–7721. doi:10.1021/ja060680r

[76] Esteves IAAC, Cruz FJAL, Müller EA, Agnihotri S, Mota JPB. Determination of the surface area and porosity of carbon nanotube bundles from a Langmuirian analysis of sub- and supercritical adsorption data. Carbon. 2009; 47:948–956. doi:10.1016/j.carbon.2008.11.044.

[77] Pérez-Ramírez EE, de la Rosa-Álvarez G, Salas P, Velasco-Santos C, Martínez-Hernández A L. Comparison as effective photocatalyst or adsorbent of carbon materials of one, two, and three dimensions for the removal of reactive red 2 in water. Environmental Engineering Science. 2015; 32:872–880. doi:10.1089/ees.2015.0083.

[78] Ren X, Chen C, Nagatsu M, Wang X. Carbon nanotubes as adsorbents in environmental pollution management: A review. Chemical Enginering Journal. 2011; 170:395–410. doi:10.1016/j.cej.2010.08.045.

[79] Smith SC, Ahmed F, Gutierrez KM, Rodrigues DF. A comparative study of lysozyme adsorption with graphene, graphene oxide, and single-walled carbon nanotubes: Potential environmental applications. Chemical Engineering Journal. 2014; 240:147–154.

[80] Apul OG, Wang Q, Zhou Y, Karanfil T. Adsorption of aromatic organic contaminants by graphene nanosheets: Comparison with carbon nanotubes and activated carbon. Water Research. 2013; 47:1648–1654. doi:10.1016/j.watres.2012.12.031

[81] Balamurugan K, Subramanian V. Adsorption of chlorobenzene onto (5,5) armchair single-walled carbon nanotube and graphene sheet: Toxicity versus adsorption strength. Journal Physical Chemistry C. 2013; 117:21217–21227. doi:10.1021/jp403646h

IntechOpen